



ELSEVIER

Available online at [www.sciencedirect.com](http://www.sciencedirect.com)

SCIENCE @ DIRECT®

International Journal of Solids and Structures 43 (2006) 3324–3336

INTERNATIONAL JOURNAL OF  
**SOLIDS and  
STRUCTURES**[www.elsevier.com/locate/ijsolstr](http://www.elsevier.com/locate/ijsolstr)

## Stochastic poromechanical modeling of anthropogenic land subsidence

Massimiliano Ferronato <sup>a,\*</sup>, Giuseppe Gambolati <sup>a</sup>,  
Pietro Teatini <sup>a</sup>, Domenico Baù <sup>b</sup>

<sup>a</sup> *Department of Mathematical Methods and Models for Scientific Applications, University of Padova,  
via Belzoni 7, 35131 Padova, Italy*

<sup>b</sup> *Department of Geological Engineering and Sciences, Michigan Technological University,  
1400 Townsend Drive, Houghton, MI, USA*

Received 18 February 2005; received in revised form 30 June 2005

Available online 12 September 2005

---

### Abstract

A key issue in poromechanical modeling, e.g. for predicting anthropogenic land subsidence due to fluid withdrawal, is the evaluation and use of representative mechanical properties for the deforming porous medium at a regional scale. One such property is the vertical uniaxial rock compressibility  $c_M$  which can be obtained through either laboratory oedometer tests or in situ measurements, and typically exhibits quite a marked scattering. This paper addresses the influence of the  $c_M$  uncertainty on the predicted land settlement using a stochastic simulation approach where  $c_M$  is regarded as a random variable and a large number of equally likely  $c_M$  realizations are generated and implemented into a poroelastic finite element model. A compressibility law, characterized by a log-normal distribution with depth-dependent mean, constant variance and exponential covariance, is assumed. The Monte Carlo simulation provides a set of responses which can be analyzed statistically. The results from a number of numerical experiments show how the  $c_M$  variance and covariance affect the reliability of the simulated land subsidence and provide a quantitative evaluation of the intrinsic uncertainty of the model prediction.

© 2005 Elsevier Ltd. All rights reserved.

*Keywords:* Stochastic compressibility; Land subsidence; Finite elements; Monte Carlo simulation

---

\* Corresponding author. Tel.: +39 049 8275929; fax: +39 049 8275995.

E-mail address: [ferronat@dmsa.unipd.it](mailto:ferronat@dmsa.unipd.it) (M. Ferronato).

URL: <http://www.dmsa.unipd.it/~ferronat> (M. Ferronato).

## 1. Introduction

Anthropogenic land subsidence due to the production of subsurface fluids, such as oil, gas, or water, has been observed worldwide over the last few decades. Well-known examples of subsidence above compacting oil fields may be found for instance in Long Beach, California (Colazas and Strehle, 1995), in Venezuela (Finol and Sancevic, 1995), or in the North Sea Ekofisk field (Hermansen et al., 2000). In Italy the Northern Adriatic coastland has experienced a pronounced settlement due to both groundwater and gas removal (e.g. Gambolati et al., 1974, 1991; Baù et al., 2001).

The need for a more reliable prediction of the impact that the development of subsurface reservoirs may have on the ground surface has led to a continuous improvement of the numerical tools employed in poromechanics. At present the use of advanced models for the most accurate prediction of land subsidence can be considered quite a common effort (Ferronato et al., 2005; Gambolati et al., *in press*). However, although sophisticated poro-visco-plastic constitutive models have been developed for a realistic description of the actual soil behavior (e.g. Alonso et al., 1990; Coussy et al., 1998; Barthelemy and Dormieux, 2002), the geomechanical analysis over producing fields is usually performed at the macroscale, with the reservoir being regarded as a homogeneous structure from a mechanical point of view and the solution to the poro-elasto-plastic equations addressed deterministically. By distinction, the importance of describing the heterogeneous nature of the subsurface has been somewhat definitely recognized in the simulation of several geohydrodynamical processes. To overcome the limits of a deterministic approach, which would require an extensive medium characterization neither supported by the available data nor allowed by the available resources, the rock hydraulic heterogeneity at the field and regional scale has been incorporated stochastically into geostatistical models (Dagan, 1989; Gelhar, 1993). While the geostatistical approach has been extensively used over the last few decades for modeling flow and transport in random porous media, a limited number of works have addressed the influence of stochastic rock heterogeneity on stress and displacements (e.g. Darrag and Tawil, 1993; Griffith and Fenton, 2001; Frias et al., 2004). In particular, to our knowledge no study has been performed on the stochastic analysis of geomechanically heterogeneous porous media using actual field observations.

A most fundamental geomechanical parameter controlling the compaction caused by pore pressure drawdown in a depleted formation is the vertical uniaxial rock compressibility  $c_M$ . The parameter  $c_M$  is often measured in the laboratory on samples with a few centimeter size taken from exploratory wells, but many difficulties may arise when upscaling such data to the field macroscale. An alternative and promising technique relies on the measurement of the in situ compaction during the field production life by the radioactive marker technique. Originally developed more than 30 years ago (De Loos, 1973), the marker records allow for a straightforward rock mechanical characterization by relating the measured compaction to the pore pressure drawdown experienced by the depleted formation. Since 1992, the radioactive marker technique has been implemented by Eni-E&P, the Italian national oil company, in several offshore boreholes of the Northern Adriatic Sea (see Fig. 1), in order to derive a most reliable assessment of  $c_M$ . Marker data processing has provided a constitutive law of  $c_M$  at the basin scale in both the first and the second loading cycle (Baù et al., 2002). The significant scattering of the original measurements, however, required a statistical analysis, based on the weighted moving average method and on a logarithmic regression, with fairly large confidence intervals.

The present paper addresses the impact of the  $c_M$  uncertainty on the predicted land subsidence using a stochastic simulation approach where  $c_M$  is regarded as a spatial random variable. Experience suggests that in normally pressurized and consolidated sedimentary basins the rock mechanical properties usually exhibit a low horizontal variability and primarily depend on depth. Since the data from the Northern Adriatic basin fulfil such a requirement (Baù et al., 2002),  $c_M$  is assumed to vary with depth only. A stochastic 1-D ergodic process for the  $c_M$  generation is implemented into a Finite Element (FE) 3-D axial-symmetric poro-elastic model solved by a Monte Carlo simulation to predict anthropogenic land subsidence due to fluid

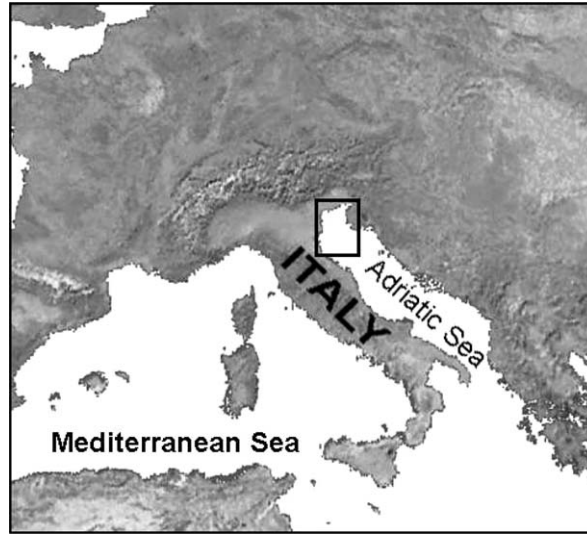


Fig. 1. The Mediterranean Sea. The geographic location of the Northern Adriatic basin is indicated by the panel.

withdrawal. It is worth noting that the 1-D stochastic generation of  $c_M$ , suggested by field observations, does not detract from the three-dimensionality of the analysis. Several numerical examples are discussed for a hydro-geological setting similar to that of the Northern Adriatic basin. A sensitivity analysis to the vertical  $c_M$  covariance, medium permeability and depth of the depleted formation is then performed. Finally, some conclusions are provided in order to describe the influence of the  $c_M$  stochastic characterization on the reliability of the predicted land subsidence and the potential of the proposed approach to address the geomechanical medium uncertainty of macroscale regional models.

## 2. Stochastic compressibility

The  $c_M$  value provided by the  $i$ th pair of markers located within a producing formation is estimated as

$$c_{M,i} = \frac{\Delta s_i}{s_{i,0} \Delta p_i} \quad (1)$$

where  $\Delta s_i$  is the shortening of the  $i$ th spacing due to the pore pressure drawdown  $\Delta p_i$ , and  $s_{i,0}$  is the initial distance between the markers, i.e. about 10.5 m (Mobach and Gussinklo, 1994). Each  $c_{M,i}$  value given by Eq. (1) can be associated to the vertical effective stress  $\sigma_{z,i}$  at the average depth of the  $i$ th spacing, with the pairs  $(c_{M,i}; \sigma_{z,i})$  thus obtained regressed to derive a constitutive relationship for the uniaxial vertical compressibility. Several  $\Delta s_i$  values are obtained during each monitoring survey in order to offset as much as possible instrumental and operational errors, so the corresponding set of  $c_{M,i}$  values can be regarded as a sample from a statistical population of data. Hence each compressibility estimate is provided as an average value  $\overline{c_{M,i}}$  with its standard deviation  $\sigma_{c_{M,i}}$ . Because of the large spatial variability of the original data, groups of adjacent measurements can be clustered together using the weighted moving average technique (Baù et al., 1999), thus allowing for narrower confidence intervals.

The analysis of the data distribution on an arithmetic plot reveals that the  $\overline{c_{M,i}}$  values follow a non-linear trend. In particular the regression by a power law provides the best correlation index, so the constitutive relationship for the uniaxial compressibility takes on the general form

$$c_M = a\sigma_z^b \quad (2)$$

The regression by a power law is equivalent to a linear regression on a double log–log plot, i.e. a linear regression carried on the population of the logarithms of the data (Hald, 1952)

$$y(x) = \alpha + \beta(x - \bar{x}) \quad (3)$$

where  $y$  and  $x$  are the logarithmic transformation of  $c_M$  and  $\sigma_z$ , respectively, and  $\bar{x}$  is the weighted mean of the  $x_i$  values. It should be noted that appropriate formulas must be used to transform the statistical population of the average  $\overline{c_{M,i}}$  with the standard deviation  $\sigma_{c_{M,i}}$  into the logarithms  $\overline{y_i}$  and  $\sigma_{y_i}$  (Papoulis, 1965).

Eq. (3) provides the mean value for  $y$ . The empirical variance  $v^2$  of the regressed  $y$  data is given by (Hald, 1952)

$$v^2 = \frac{\sum_{i=1}^N [\overline{y_i} - y(x_i)]^2}{N - 2} \quad (4)$$

with  $N$  the total number of regressed values. Hence, the 95% confidence interval for  $y$  is obtained as

$$y = \alpha - \beta\bar{x} + \beta x \pm 2v \quad (5)$$

Back transformation of (5) to  $c_M$  provides

$$c_M = 10^{\alpha - \beta\bar{x} + 2v} \sigma_z^\beta \quad (6)$$

and comparison between Eqs. (2) and (6) shows that the power law coefficients  $a$  and  $b$  read

$$a = 10^{\alpha - \beta\bar{x} + 2v} \quad (7)$$

$$b = \beta \quad (8)$$

The above procedure has been used by Baù et al. (2002) to derive a constitutive relationship for  $c_M$  in the Northern Adriatic basin. The regression of the data obtained from 11 marker surveys in 3 instrumented boreholes during the period 1992–1999 provided the following constitutive model:

$$c_M = 1.0044 \times 10^{-2} \sigma_z^{-1.1347} \quad (9)$$

where  $c_M$  represents the expected (mean) value of the uniaxial compressibility. The 95% confidence interval, corresponding to  $-2v$  and  $+2v$  in Eq. (6), is defined by  $a = 5.1602 \times 10^{-3}$  and  $1.9546 \times 10^{-2}$ , respectively. In Eq. (9)  $c_M$  is in [MPa<sup>-1</sup>] and  $\sigma_z$  in [MPa]. A graphical representation of (9) is given in Fig. 2.

By the way it is calculated (see Eq. (7)), coefficient  $a$  of Eq. (2) is a log-normally distributed random variable with mean value and variance given by (Hald, 1952)

$$E(\log a) = \log \mu = \alpha - \beta\bar{x} \quad (10)$$

$$E[(\log a - \log \mu)^2] = \sigma^2 = v^2 \quad (11)$$

where  $\alpha$ ,  $\beta$ , and  $\bar{x}$  are obtained from the regression (Eq. (3)) of the available sample of data, and  $v^2$  is calculated by Eq. (4). The coefficient  $b$  (see Eq. (8)) is directly obtained from the regression procedure. For the Northern Adriatic basin, Eqs. (10) and (11) provide  $\log \mu = -1.9981$ , with  $\beta = -1.1347$  and  $\sigma^2 = 0.0209$ .

The vertical effective stress  $\sigma_z$  in undisturbed conditions can be calculated as a function of the depth  $z$ . Using Terzaghi's effective stress principle (Terzaghi and Peck, 1967), we have

$$\sigma_z = \hat{\sigma}_z - p \quad (12)$$

where  $\hat{\sigma}_z$  is the total vertical stress (compressive stresses are assumed to be positive). The total vertical stress can be calculated by means of the overburden gradient function  $\text{obg}(z)$ , defined such that  $\hat{\sigma}_z = z \cdot \text{obg}(z)$ . Assuming the basin to be normally pressurized and fully saturated with groundwater, the pore fluid pressure is calculated as  $\gamma_w z$ , where  $\gamma_w$  is the groundwater specific weight. Finally, Eq. (12) becomes

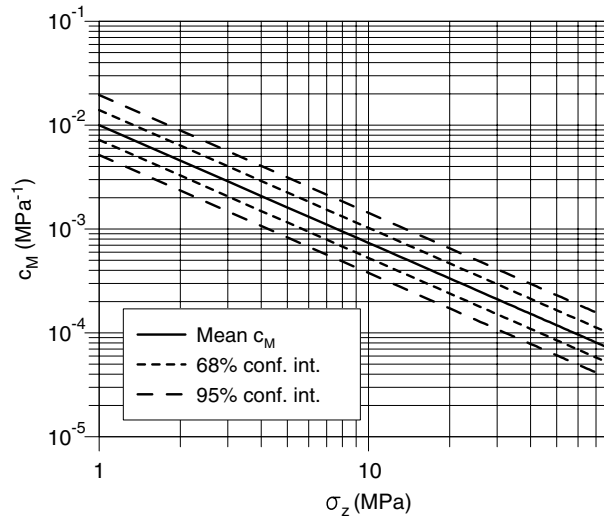


Fig. 2. Constitutive model of the vertical uniaxial compressibility for the Northern Adriatic basin (after Baù et al. (2002)). The dashed profiles show the 68% and 95% confidence intervals on a double log–log plot.

$$\sigma_z = [\text{obg}(z) - \gamma_w]z \quad (13)$$

For the Northern Adriatic basin an average overburden gradient function has been estimated by density log surveys yielding the following expression for Eq. (13) (Baù et al., 2002):

$$\sigma_z = (1.2218 \times 10^{-2} \cdot z^{0.0766} - 9.8 \times 10^{-3})z \quad (14)$$

In Eq. (14)  $z$  is in [m] and  $\sigma_z$  in [MPa]. Using  $\sigma_z$  from Eq. (14) in (9) allows for the calculation of  $c_M$  as a function of depth  $z$  only, so that  $c_M$  can be assumed to be constant within any horizontal layer.

In the analysis that follows, an ensemble of equally likely spatial distributions of  $c_M$  is obtained by assuming  $a$  as a linear (function of  $z$  only), stationary, and ergodic stochastic process (de Marsily, 1986), characterized by a log-normal distribution with mean value and variance as defined in Eqs. (10) and (11). The stochastic realizations of  $a$  are generated using the method of Rice (1954) as modified by Shin-ozuka and Jan (1972), and assuming an exponential covariance function

$$\text{cov}[\log a(z_1), \log a(z_2)] = \sigma^2 \cdot \exp\left(-\frac{|z_1 - z_2|}{\lambda}\right) \quad (15)$$

where  $\lambda$  is the vertical correlation length.

### 3. Numerical experiments

The ensemble of spatial realizations of  $c_M$  generated with the correlated random line process are used in a test case to simulate land subsidence by a Monte Carlo simulation. The problem concerns a cylindrical porous volume with a radius of 8000 m and a height of 5000 m consisting of a sequence of alternating sandy and clayey layers with hydro-geological properties typical of the Northern Adriatic basin. Hydraulic conductivity of sand ( $k_{\text{sand}}$ ) and clay ( $k_{\text{clay}}$ ) is assumed to decrease with depth from  $10^{-5}$  to  $10^{-7}$  m/s, and from  $10^{-9}$  to  $10^{-11}$  m/s, respectively (Ferronato et al., 2004). The Poisson ratio  $\nu$  is set to 0.3 (Teatini et al., 2000) and the grain compressibility to  $1.63 \times 10^{-5}$   $\text{MPa}^{-1}$  (Geertsma, 1973). The lower boundary is fixed and

impervious; the lateral boundary is fixed, too, with a zero pore pressure variation enforced on it. At the ground surface zero external stress and zero incremental pore pressure are prescribed (Baù et al., 2004).

A pumping of 1000 m<sup>3</sup>/day, evenly distributed over a cylindrical volume with radius equal to 500 m, is assumed to take place from a sandy layer 20 m thick and 1000 m deep. In the present study we address land subsidence at the steady state, so that the problem is uncoupled with the pore pressure solution independent of  $c_M$ . Hence the incremental pressure field  $p$  is provided by the deterministic solution to the classical steady state flow equation

$$\nabla \left[ K_{ij} \left( \frac{\nabla p}{\gamma_w} \right) \right] = f \tag{16}$$

where  $K_{ij}$  are the components of the hydraulic conductivity tensor and  $f$  the forcing source/sink function. The stochastic solution to the poromechanical problem is obtained in terms of the displacements  $\mathbf{u} = (u_x, u_y, u_z)^T$  by solving the equations of equilibrium for an isotropic, generally heterogeneous, porous medium

$$G \nabla^2 u_i + (A + G) \frac{\partial(\text{div } \mathbf{u})}{\partial i} = \frac{\partial p}{\partial i} \quad i = x, y, z \tag{17}$$

where the shear modulus  $G$  and the Lamé constant  $A$  are random variables related to  $c_M$  through the following:

$$G = \frac{1 - 2\nu}{2(1 - \nu)c_M} \tag{18}$$

$$A = \frac{\nu}{(1 - \nu)c_M} \tag{19}$$

The test problem is solved using an axi-symmetric configuration. The porous volume is discretized into annular elements with a 3-node triangular cross-section, totalizing 8096 nodes, 15834 elements, and 87 horizontal layers with thickness ranging between 10 and 250 m. The mesh structure is shown in Fig. 3 along with the boundary conditions imposed on displacements. The pore pressure field at steady state is obtained

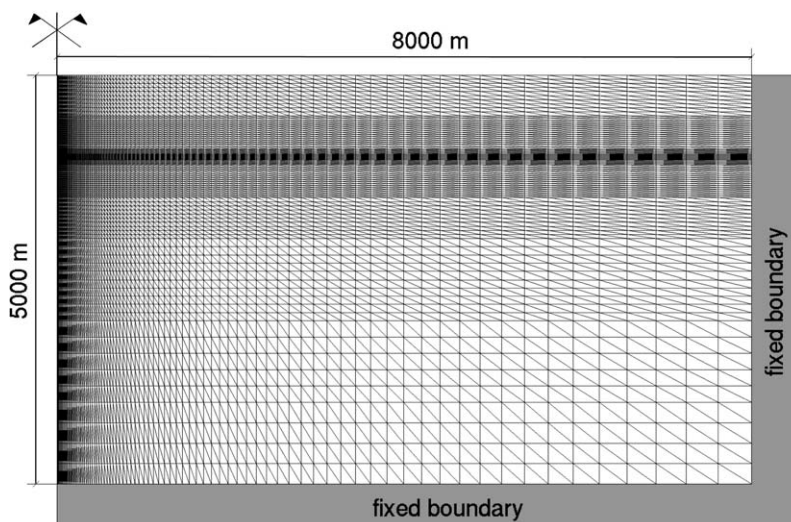


Fig. 3. Vertical cross-section of the FE mesh with the displacement boundary conditions.



by solving the flow equation (16) in a cylindrical reference frame via the FE method. The average pore pressure drawdown within the pumped volume turns out to be about 1.5 MPa. The pore pressure field thus obtained is used as an external source of strength in Eqs. (17) solved by FE with the total stress formulation (Gambolati et al., 2001) for each of the generated spatial realizations of  $c_M$ .

The stochastic simulation is performed using an ensemble of 1000  $c_M$  realizations, with each  $c_M$  distribution generated over a vertical step of 5 m. For layers thicker than 5 m  $c_M$  is computed as the mean of the compressibility values comprised within those layer. An example of the difference between the original distribution of  $c_M$  generated every 5 m and the actual values used in the discretized FE layers of Fig. 3 is shown in Fig. 4. The number of  $c_M$  spatial realizations (1000) proves sufficiently large so as to reproduce at the mid-depth of each layer the average (expected) value and the 95% confidence interval prescribed by the constitutive law (9).

Since the  $c_M$  values are log-normally distributed because of the definitions of  $a$  and  $b$  (Eqs. (7) and (8)), and the displacement in a poroelastic model is linearly dependent on  $c_M$ , land subsidence is also expected to be log-normally distributed. The frequency distribution obtained with the Monte Carlo simulation is compared to the theoretical log-normal Probability Distribution Function (PDF) (Hald, 1952)

$$\phi(\eta) = \frac{M}{\sigma\eta} \varphi(u) \tag{20}$$

with  $M = \log e = 0.4343$ ,  $\eta$  land subsidence, and  $\varphi(u)$  the normal distribution function

$$\varphi(u) = \frac{1}{\sqrt{2\pi}\sigma} e^{-\frac{u^2}{2}} \quad u = \frac{\log \eta - \log \mu}{\sigma} \tag{21}$$

Fig. 5 shows this comparison, assuming a correlation length  $\lambda$  (Eq. (15)) equal to 50 m, for two points located on the top surface, one at the symmetry axis ( $r = 0$ , maximum subsidence) and the other over the outer boundary of the depleted cylindrical volume ( $r = 500$  m). As expected, land subsidence fits quite well into a log-normal distribution and the size of the confidence intervals decreases as we move farther from the symmetry axis.

An additional piece of information provided by the stochastic approach is the probability that at some points of particular interest the expected subsidence will exceed a limit threshold value  $\eta_t$ . As is well known, the probability that  $\eta > \eta_t$  is obtained by integrating over the point of interest the PDF between  $\eta_t$  and  $+\infty$

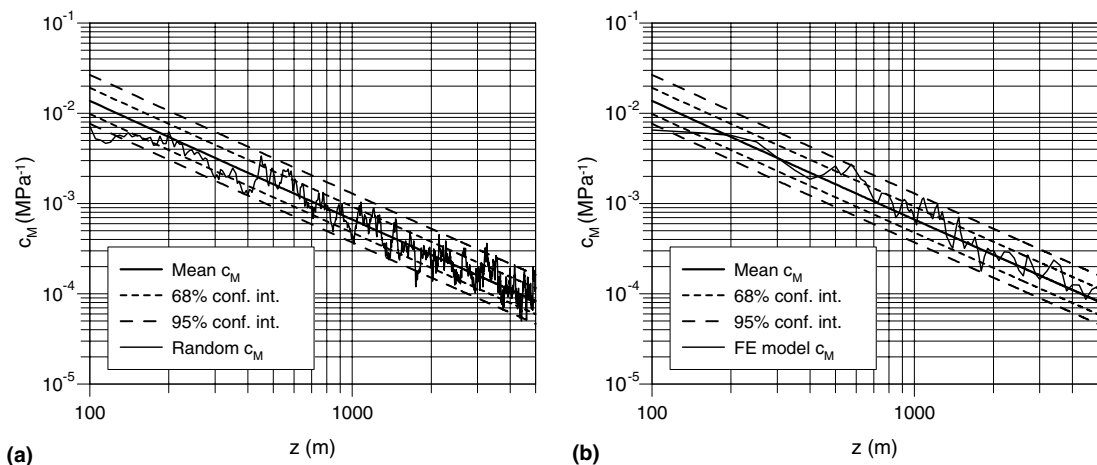


Fig. 4. Example of a stochastic realization for  $c_M$  obtained with  $\lambda = 50$  m: (a)  $c_M$  values generated every 5 m; (b)  $c_M$  values prescribed in each mesh layer.

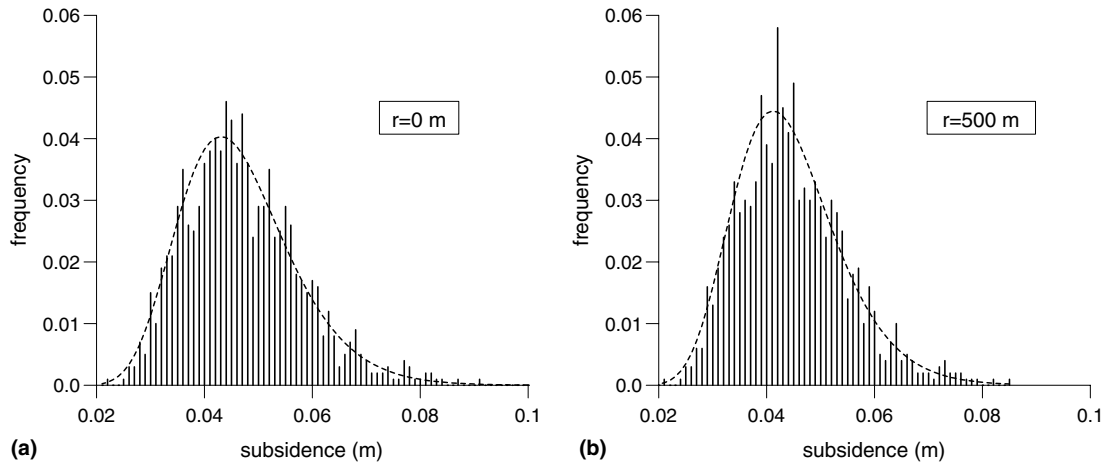


Fig. 5. Frequency plot (linebars) and theoretical (dashed profile) PDF of land subsidence at: (a) surface point with maximum subsidence ( $r = 0$  m); (b) surface point over the outer boundary of the depleted cylindrical volume ( $r = 500$  m).

$$P(\eta > \eta_t) = \int_{\eta_t}^{+\infty} \phi(\eta) d\eta \tag{22}$$

As an example, consider as a threshold value  $\eta_t = 5$  cm. At  $r = 0$ , the mean value for  $\eta$  is 4.65 cm and the 95% confidence interval is  $2.88 < \eta < 7.14$  cm. The probability of exceedance  $P(\eta > \eta_t)$  turns out to be 34%. At  $r = 2000$  m, for instance, where the mean value for  $\eta$  is 3.00 cm and the 95% confidence interval is  $2.02 < \eta < 4.32$  cm,  $P(\eta > \eta_t)$  turns out to be only 0.1%.

### 3.1. Sensitivity analysis

To gain a better insight on the impact of the  $c_M$  uncertainty on the land subsidence prediction in different field conditions, a sensitivity analysis has been performed for the following parameters:

- (1) the correlation length  $\lambda$ ;
- (2) the permeability contrast  $\kappa = k_{\text{sand}}/k_{\text{clay}}$ ;
- (3) the pumped aquifer depth  $h$ .

#### 3.1.1. Correlation length

The influence of the correlation length  $\lambda$  is studied for the limiting cases  $\lambda \rightarrow 0$  and  $\lambda \rightarrow \infty$ . An example of the generated random  $c_M$  vs.  $z$  for various  $\lambda$  values is provided in Fig. 6 which helps understand how the correlation length affects the  $c_M$  realizations. The 95% confidence intervals for the predicted land subsidence are given in Fig. 7 along with the subsidence profiles obtained from the  $c_M$  constitutive law of Eq. (9) with  $a = 1.0044 \times 10^{-2}$  (mean value), and  $a = 5.1602 \times 10^{-3}$  and  $1.9546 \times 10^{-2}$  (95% confidence interval limits). When  $\lambda \rightarrow 0$ , practically obtained by setting  $\lambda = 1$  m, the  $c_M$  in adjacent layers is not correlated and the 95% confidence interval turns out to be quite narrow. By contrast, as  $\lambda \rightarrow \infty$ , practically obtained by setting  $\lambda > 10000$  m, all  $c_M$  are correlated and the stochastic simulation provide almost the same 95% confidence interval as the one obtained with the extreme profiles of Fig. 2. The latter turns out to be the most conservative assumption, as it provides the largest confidence interval.



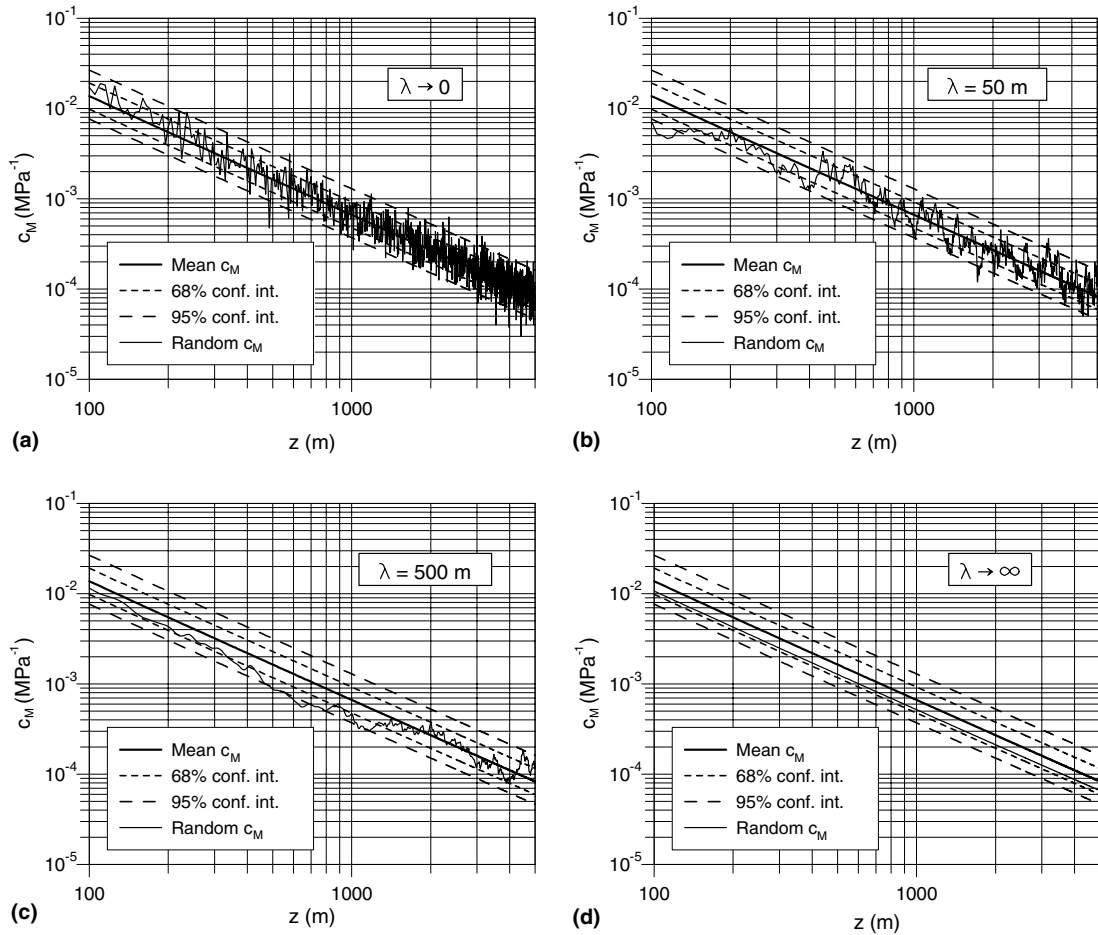


Fig. 6. Examples of  $c_M$  stochastic realizations with: (a)  $\lambda \rightarrow 0$  m; (b)  $\lambda = 50$  m; (c)  $\lambda = 500$  m; (d)  $\lambda \rightarrow \infty$ .

### 3.1.2. Permeability contrast

The hydraulic conductivity assumed for sand and clay in each test problem is summarized in Table 1 along with the ratio  $\kappa$ . Groundwater withdrawal is calibrated so as to achieve in any case a maximum pore pressure drawdown approximately equal to 1.5 MPa within the pumped sandy formation. Hence, the effect of decreasing  $\kappa$  is that of increasing the volume of the depleted porous medium, as is shown in Fig. 8 which provides the extent of the steady state drawdown in three test cases around the pumped aquifer.

The results obtained from the Monte Carlo simulation with  $\lambda = 50$  m are shown in Fig. 9. To perform a meaningful comparison, land subsidence  $\eta(r)$  is normalized with respect to  $\bar{\eta}(r)$ , i.e. the mean value at the radial distance  $r$ . Fig. 9a suggests that the prediction uncertainty, as quantified by the amplitude of the 95% confidence interval, decreases as a larger porous volume is depleted. This is further evidenced in Fig. 9b, where narrower PDFs of the normalized land subsidence at  $r = 0$  correspond to smaller  $\kappa$  values. This behavior is due to the fact that land subsidence primarily depends on the compaction of the depleted medium. For smaller  $\kappa$ , the overall compaction is controlled by the  $c_M$  of a larger set of adjacent layers and, as is known from statistics, the size of the corresponding confidence interval decreases as the number of random values within the group increases.

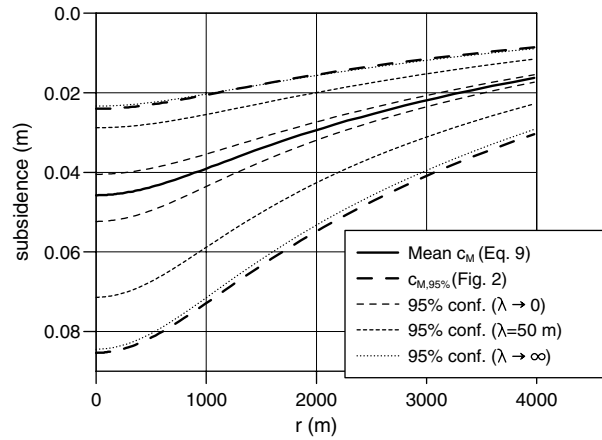


Fig. 7. Land subsidence obtained with mean  $c_M$  and the most extreme profiles of Fig. 2 (thick profiles), and land subsidence obtained with the Monte Carlo simulation (thin profiles) and different  $\lambda$ .

Table 1

Hydraulic conductivity of sand and clay in the numerical test problems. The ratio  $k_{\text{sand}}/k_{\text{clay}}$  is denoted by  $\kappa$

	$k_{\text{sand}}$ [m/s]	$k_{\text{clay}}$ [m/s]	$\kappa$
Base case	$10^{-5}$ – $10^{-7}$	$10^{-9}$ – $10^{-11}$	10000
$k_1$	$10^{-5}$ – $10^{-7}$	$10^{-8}$ – $10^{-10}$	1000
$k_2$	$10^{-5}$ – $10^{-7}$	$10^{-7}$ – $10^{-9}$	100

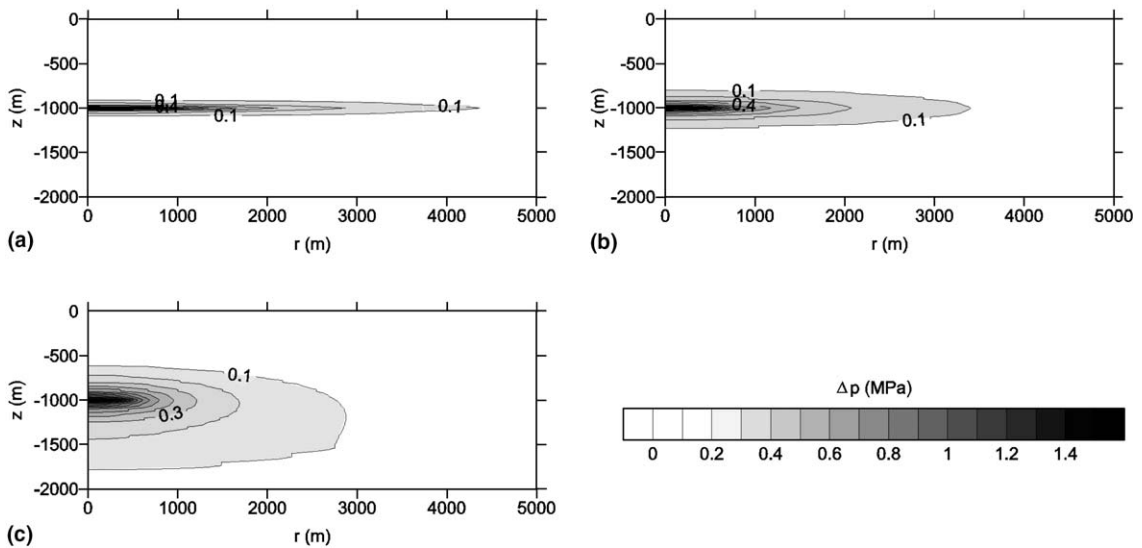


Fig. 8. Pore pressure drawdown (in MPa) for the test cases: (a) base case; (b)  $k_1$ ; (c)  $k_2$ . Groundwater pumping is calibrated so as to attain a maximum pore pressure drawdown of 1.5 MPa.

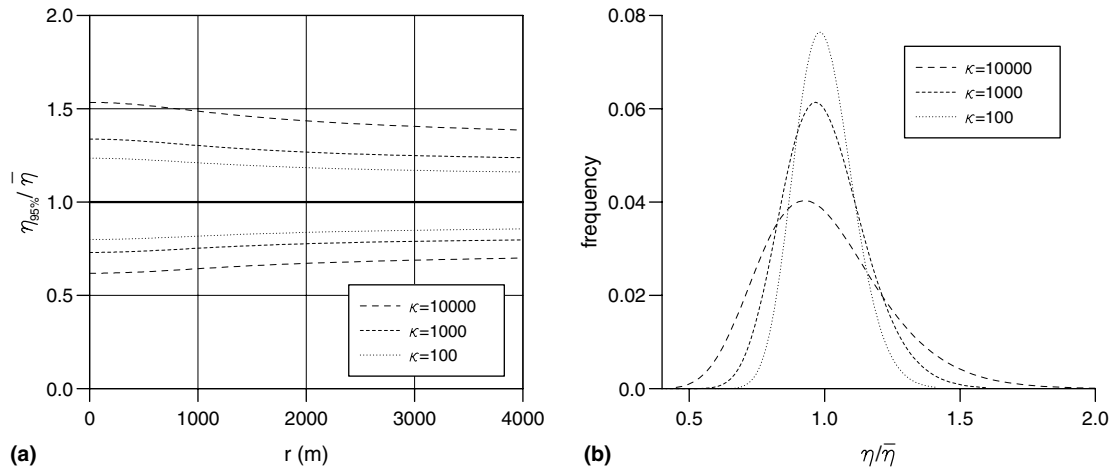


Fig. 9. (a) 95% confidence intervals of the normalized land subsidence obtained with the Monte Carlo simulation and different  $\kappa$  values; (b) PDF of the normalized land subsidence at the symmetry axis.

### 3.1.3. Aquifer depth

Two further examples are discussed by using a pumped aquifer depth  $h$  of 500 m and 2000 m. As was done previously, the normalized land subsidence  $\eta(r)/\bar{\eta}(r)$  is considered in order to compare meaningfully the different test cases. Fig. 10 points to a very small difference among the test cases, with an almost negligible decrease of the 95% confidence interval size as  $h$  increases. This is accounted for by the general form of Eq. (2), where  $a$  is the actual stochastic parameter with constant mean and variance. As  $h$  increases,  $\sigma_z$  increases too and  $\sigma_z^b$  decreases, being the exponent  $b$  negative. The most notable consequence is that the size of the confidence interval associated with  $c_M$  decreases with depth, hence a reduced uncertainty is expected as the depth of the depleted formation increases. Because of the exponential form of (2), however, such a variation is very small for the depth of usual interest. Thus we can conclude that the depth  $h$  plays a

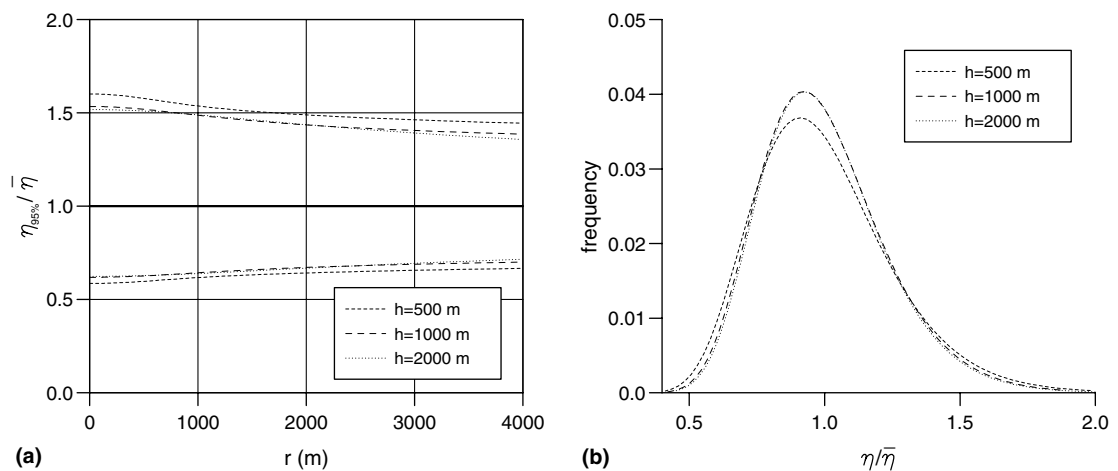


Fig. 10. (a) 95% confidence intervals of the normalized land subsidence obtained with the Monte Carlo simulation and different  $h$  values; (b) PDF of the normalized land subsidence at the symmetry axis.

negligible role on the uncertainty of  $\eta$  as is related to the stochastic geomechanical properties of the porous medium.

#### 4. Conclusions

The present paper addresses the influence of the geomechanical uncertainty of the porous medium on the prediction of anthropogenic land subsidence due to subsurface fluid withdrawal. The study focuses on the vertical uniaxial rock compressibility  $c_M$  and uses a stochastic approach where  $c_M$  is regarded as a random spatial process. An axi-symmetric aquifer system is simulated with a stratified hydro-geological setting typical of a sedimentary basin with the geomechanical properties taken from the Northern Adriatic, Italy. A basin-scale constitutive law for  $c_M$ , log-normally distributed with depth-dependent mean and constant variance, is derived from the statistical analysis of available in situ marker measurements (Baù et al., 2002) and implemented into a poroelastic stochastic FE model based on a Monte Carlo simulation of an ensemble of 1000 realizations.

A sensitivity analysis to the  $c_M$  vertical correlation length, permeability contrast between sand and clay, and depleted aquifer depth is performed. The following results are worth summarizing:

- the correlation length  $\lambda$  has a significant impact on the amplitude of the 95% confidence interval, which increases as also  $\lambda$  increases. In the limiting case with  $\lambda \rightarrow \infty$  the largest confidence interval is obtained, i.e. the one derived by Baù et al. (2002);
- a larger permeability contrast helps reduce the volume of the depleted porous medium, and hence increase the uncertainty of the resulting land subsidence;
- the uncertainty of land subsidence prediction proves almost insensitive to the aquifer depth.

Finally, the results point out that the  $c_M$  stochastic characterization may help define the quality of the simulation and represent a first contribution to the evaluation of the geomechanical uncertainty on the reliability of the predicted land subsidence. New on-going research is addressing the influence of the  $c_M$  uncertainty on the transient land subsidence where the flow field is also affected by the geomechanical response of the porous medium.

#### Acknowledgement

This study has been partially funded by the Italian MIUR project “Numerical Methods and Algorithms for Environmental Modeling”.

#### References

- Alonso, E.E., Gens, A., Josa, A., 1990. A constitutive model for partially saturated soils. *Géotechnique* 40, 405–430.
- Barthelemy, J.F., Dormieux, L., 2002. Micromechanical approach to the modelling of compaction at large strains. In: Auriault, L.L. et al. (Eds.), *Poromechanics II*. A.A. Balkema Publishers, Amsterdam, pp. 99–105.
- Baù, D., Gambolati, G., Teatini, P., 1999. Statistical analysis of in situ compaction measurements for anthropogenic land subsidence prediction in the Northern Adriatic basin. In: Lippard, A.N.S.J., Sinding-Larsen, R. (Eds.), *Proceedings of the 5th Conference of the International Association of Mathematical Geology*, vol. 1. Tapir Publishers, Trondheim, pp. 299–304.
- Baù, D., Ferronato, M., Gambolati, G., Teatini, P., 2001. Land subsidence spreading factor of the Northern Adriatic gas fields, Italy. *International Journal of Geomechanics* 1, 459–475.
- Baù, D., Ferronato, M., Gambolati, G., Teatini, P., 2002. Basin-scale compressibility of the Northern Adriatic by the radioactive marker technique. *Géotechnique* 52, 605–616.

- Baù, D., Ferronato, M., Gambolati, G., Teatini, P., 2004. Surface flow boundary conditions in modelling land subsidence due to fluid withdrawal. *Ground Water* 42, 516–525.
- Colazas, X.C., Strehle, R.W., 1995. Subsidence in the Wilmington oil field, Long Beach, California, USA. In: Chilingarian, G.W., Donaldson, E.C., Yen, T.F. (Eds.), *Subsidence due to Fluid Withdrawal*. Elsevier Science, Amsterdam, pp. 285–335.
- Coussy, O., Dormieux, L., Detournay, E., 1998. From mixture theory to Biot's approach for porous media. *International Journal of Solids and Structures* 35, 4619–4635.
- Dagan, G., 1989. *Flow and Transport in Porous Formations*. Springer-Verlag, Berlin.
- Darrag, A., Tawil, M., 1993. The consolidation of soils under stochastic initial pore pressures. *Applied Mathematical Modelling* 17, 609–612.
- De Loos, J.M., 1973. In situ compaction measurements in Groningen observation wells. *Verhandelingen van het Koninklijk Nederlands geologisch mijnbouwkundig Genootschap* 28, 79–104.
- de Marsily, G., 1986. *Quantitative Hydrology: Groundwater Hydrology for Engineers*. Academic Press, Inc., New York.
- Ferronato, M., Gambolati, G., Teatini, P., Baù, D., 2004. Radioactive marker measurements in heterogeneous reservoirs: numerical study. *International Journal of Geomechanics* 4, 79–92.
- Ferronato, M., Gambolati, G., Pini, G., Teatini, P., 2005. Computational issues in anthropogenic land subsidence prediction. In: Barla, G., Barla, M. (Eds.), *Prediction, Analysis and Design in Geomechanical Applications, Proceedings of the 11th International Conference on Computer Methods and Advances in Geomechanics*, vol. 4. Patron Editore, Bologna, pp. 297–306.
- Finol, A.S., Sancevic, Z.A., 1995. Subsidence in Venezuela. In: Chilingarian, G.W., Donaldson, E.C., Yen, T.F. (Eds.), *Subsidence due to Fluid Withdrawal*. Elsevier Science, Amsterdam, pp. 337–372.
- Frias, D.G., Murad, M.A., Pereira, F., 2004. Stochastic computational modelling of highly heterogeneous poroelastic media with long-range correlations. *International Journal for Numerical and Analytical Methods in Geomechanics* 28, 1–32.
- Gambolati, G., Gatto, P., Freeze, R.A., 1974. Mathematical simulation of the subsidence of Venice. 2. Results. *Water Resources Research* 10, 563–577.
- Gambolati, G., Ricceri, G., Bertoni, W., Brighenti, G., Vuillemin, E., 1991. Mathematical simulation of the subsidence of Ravenna. *Water Resources Research* 27, 2899–2918.
- Gambolati, G., Ferronato, M., Teatini, P., Deidda, R., Lecca, G., 2001. Finite element analysis of land subsidence above depleted reservoirs with pore pressure gradient and total stress formulations. *International Journal of Numerical and Analytical Methods in Geomechanics* 25, 307–327.
- Gambolati, G., Teatini, P., Ferronato, M., in press. Anthropogenic land subsidence. In: Anderson, M.G. (Ed.), *The Encyclopedia of Hydrological Sciences*. John Wiley & Sons, London.
- Geertsma, J., 1973. Land subsidence above compacting oil and gas reservoirs. *Journal of Petroleum Technology* 25, 734–744.
- Gelhar, L., 1993. *Stochastic Subsurface Hydrology*. Prentice-Hall, New Jersey.
- Griffith, D.V., Fenton, G.A., 2001. Bearing capacity of spatially random soil: the undrained clay Prandtl problem revisited. *Géotechnique* 51, 351–359.
- Hald, A., 1952. *Statistical Theory with Engineering Applications*. John Wiley & Sons, New York.
- Hermansen, H., Landa, G.H., Sylte, J.E., Thomas, L.K., 2000. Experiences after 10 years of waterflooding the Ekofisk field, Norway. *Journal of Petroleum Science and Engineering* 26, 11–18.
- Mobach, E., Gussinklo, H.J., 1994. In situ reservoir compaction monitoring in the Groningen field. In: *Proceedings of EUROCK'94, Rock Mechanics for Petroleum Engineering*. A.A. Balkema Publ., Rotterdam, pp. 535–547.
- Papoulis, A., 1965. *Probability, Random Variables and Stochastic Processes*. McGraw-Hill, New York.
- Rice, S.O., 1954. Mathematical analyses of random noise. In: Wax, N. (Ed.), *Selected Papers on Noise and Stochastic Processes*. Dover, New York.
- Shinozuka, M., Jan, C.M., 1972. Digital simulation of random processes and its applications. *Journal of Sound and Vibration* 25, 111–128.
- Teatini, P., Baù, D., Gambolati, G., 2000. Water–gas dynamics and coastal land subsidence over Chioggia Mare field, Northern Adriatic Sea. *Hydrogeology Journal* 8, 462–479.
- Terzaghi, K., Peck, R.B., 1967. *Soil Mechanics in Engineering Practice*, second ed. John Wiley & Sons, New York, NY.